Electronic Supplementary Information

A hydrogen-bonded assembly of cucurbit[6]uril and [$MoO_2Cl_2(H_2O)_2$] with catalytic efficacy for the one-pot conversion of olefins to alkoxy products

Lucie S. Nogueira,[a] Margarida M. Antunes,[a] Ana C. Gomes,[a] Luís Cunha-Silva,[b] Martyn Pillinger,*[a] André D. Lopes,[c] Anabela A. Valente *[a] and Isabel S. Gonçalves *[a]

[a] *Ms. L. S. Nogueira, Dr. M. M. Antunes, Dr. A. C. Gomes, Dr. M. Pillinger, Dr. A. A. Valente, Prof. Dr. I. S. Gonçalves*
Department of Chemistry, CICECO - Aveiro Institute of Materials, University of Aveiro, Campus Universitário de Santiago, 3810-193 Aveiro, Portugal
E-mail: mpillinger@ua.pt (M.P.), atav@ua.pt (A.A.V.), igoncalves@ua.pt (I.S.G.)

[b] *Dr. L. Cunha-Silva*
REQUIMTE/LAQV & Department of Chemistry and Biochemistry, Faculty of Sciences, University of Porto, 4169-007 Porto, Portugal

[c] *Dr. A. D. Lopes*
CCMar, and Department of Chemistry and Pharmacy, FCT, University of the Algarve, P-8005-039 Faro, Portugal

Materials and methods

The following chemicals were purchased from Sigma-Aldrich unless otherwise indicated, and used as received: (For synthesis) Glycoluril (97%), paraformaldehyde, 37% hydrochloric acid, acetone (p.a., 99.5%, Scharlau), diethylene glycol dimethyl ether (diglyme; 99%, Fluka) and molybdenum trioxide (99.5%, Analar); (for catalysis) *cis*-cyclooctene (95%, Alfa Aesar), cyclooctene oxide (99%), cyclooctanol (97%, Alfa Aesar), *cis*-1,2-cyclooctanediol (99%), cyclohexene (99% GC, Riedel-de Haën), cyclohexene oxide (98%), cyclohexanol (>99%, Merck), styrene (≥ 97%, Fluka), 2,6-Di-tert-butyl-4-methyl phenol (≥99%), acetonitrile (≥ 99.9% Chromasolv® grade for HPLC), methanol (≥ 99.9%, Chromasolv® grade for HPLC), absolute ethanol (≥ 99.8% puriss p.a. for GC), 1-butanol (99.4% ACS, Alfa Aesar), *N*,*N*-dimethylformamide (≥ 99%), 30% aq. H_2O_2 (Riedel-de Haën) and acetone (≥ 99.5% puriss p.a., ACS reagent, Reag ISO, Reag Ph. Eur.). The complex $[MoO_2Cl_2(H_2O)_2]\cdot(diglyme)_2$ (**1**) was prepared as described previously and gave concordant elemental analysis, FT-IR and ^1H NMR data.[1]

Elemental analyses for C, H, and N were obtained using a Leco TruSpec 630-200-200 analyzer. TGA was performed using a Shimadzu TGA-50 thermobalance system at a heating rate of 5 °C min^{-1} to 800 °C under air. N_2 adsorption isotherms at −196 °C were measured using a Quantachrome instrument (automated gas sorption data using Autosorb IQ$_2$). The samples were pre-treated at 80 °C for 2 h under vacuum ($< 4\times10^{-3}$ bar). PXRD data were collected at ambient temperature using a Malvern Panalytical Empyrean diffractometer equipped with a PIXcel 1D detector set at 240 mm from the sample, in a Bragg-Brentano para-focusing optics configuration equipped with a spinning flat plate sample holder. Cu-K$_{\alpha1,2}$ X-radiation (λ_1 = 1.540598 Å; λ_2 = 1.544426 Å) filtered with a nickel foil was used. Working operating conditions for the X-ray tube: 45 kV and 40 mA. Intensity data were collected in continuous mode in the ca. $3.5 \leq 2\theta \leq 70°$ range. SEM images, EDS and elemental mappings of Mo, N and O were collected on a Hitachi SU-70 microscope equipped with a Bruker Quantax 400 detector operating at 15 kV. Samples were prepared by deposition on aluminium sample holders, followed by carbon coating using an Emitech K 950 carbon evaporator. Transmission FT-IR spectra were measured on a Mattson 7000 spectrometer (128 scans and resolution of 4.0 cm^{-1}) in the 300−4000 cm^{-1} range using KBr pellets. Attenuated total reflectance (ATR) FT-IR spectra were recorded on a Bruker Optics Tensor 27 instrument equipped with a Specac Golden Gate Mk II ATR accessory having a diamond top-plate and KRS-5 focusing lenses (256 scans and resolution of 4.0 cm^{-1}). FT-Raman spectra were recorded on a RFS-100 Bruker FT-Spectrometer equipped with a Nd:YAG laser with an excitation wavelength of 1064 nm. $^{13}C\{^1H\}$ CP MAS NMR spectra were recorded using a Bruker Avance 400 (narrow bore) spectrometer with an ultrashielded static magnetic field of 100.6 MHz. The spectra were recorded with 2.75 μs ^1H 90° pulses, 2.0 ms contact time, spinning rate of 14 kHz, and 5 s recycle delays. Chemical shifts are quoted in ppm from TMS.

Synthesis of CB[6]

CB[6] was prepared and purified by using a modified procedure based on those described earlier by Kim *et al.*[2] and Day *et al.*[3] A mixture of glycoluril (300 g, 2.11 mol), paraformaldehyde (135 g, 4.48 mol) and conc. HCl (300 mL) was heated at 80 °C for 150 min and then at 100 °C for 24 h. After addition of water (2.5 L), undissolved solid (CB[6] + CB[8]) was removed by filtration. The solid mixture of CB[6] + CB[8] (260 g) was mixed with 3 M HCl (3 L) during 1 h. The solution was filtered off and acetone was added to precipitate pure CB[6], which was filtered and air-dried (136 g, 31% based on glycoluril). Anal. Calcd for $C_{36}H_{36}N_{24}O_{12}\cdot 6H_2O\cdot 2.5HCl\cdot 0.9(CH_3COCH_3)$ (1248.3): C, 37.23; H, 4.51; N, 26.93. Found: C, 37.23; H, 4.61; N, 26.93. TGA (Fig. S2) revealed a weight loss of 12.5% up to 150 °C [calcd for loss of $6H_2O$ and $0.9(CH_3COCH_3)$: 12.8%].

Single crystal X-ray diffraction

Single crystals of **2** were collected and immersed in highly viscous oil (Fomblin Y, Aldrich), and a selected crystal was mounted on a CryoLoop.[4] Full diffraction data were collected on a Bruker X8 APEX II CCD area-detector diffractometer controlled by APEX2 software (Mo-K_α graphite-monochromated radiation, $\lambda = 0.71073$ Å; the crystal was distanced at 40 mm from the detector; the exposure time per frame was 15 s).[5] The temperature of acquisition, 150(2) K, was set up with an Oxford Cryosystems Series 700 cryosystem monitored by the interface Cryopad.[6] Images were processed using SAINT+,[7] and the absorption effects were corrected by the multi-scan semi-empirical method implemented in SADABS.[8] The structure was solved using SHELXT-2014.[9,10] Non-H atoms were located from difference Fourier maps calculated and refined by using anisotropic displacement from successive full-matrix least squares refinement cycles on F^2 using SHELXL-v.2014.[9,11]

H-atoms bound to carbon atoms of CB[6] were placed at geometrical positions using *HFIX* instructions in SHELXL (*23* for the CH_2 and *13* for the CH groups) and included in subsequent refinement cycles in riding-motion approximation with isotropic thermal displacement parameters (U_{iso}) fixed at 1.2 × U_{eq}. The H-atoms associated with the coordinated and fully occupied uncoordinated water molecules were markedly visible in the difference Fourier maps, and included in subsequent refinement stages with the O–H and H···H distances restrained to 0.87(1) and 1.43(2) Å, respectively, and using a riding-motion approximation with an isotropic thermal displacement parameter fixed at 1.5 × U_{eq} of the parent oxygen atom. Although the H-atoms of the partially occupied water molecules of crystallization were not located from difference Fourier maps or positioned in calculated positions, they were considered in the final molecular formula.

Table S1 summarises the main information about the crystal data, the single-crystal X-ray data collection and the structure refinement. The CIF file was deposited with the Cambridge Crystallographic Data Centre as supplementary publication data No. CCDC-1900402. Copies of the data can be obtained online at https://www.ccdc.cam.ac.uk/structures/.

Table S1 Crystal and structure refinement data for $2[MoO_2Cl_2(H_2O)_2]\cdot(C_{36}H_{36}N_{24}O_{12})\cdot 17H_2O\cdot 2HCl$ (**2**).

Chemical formula	$C_{36}H_{80}Cl_6Mo_2N_{24}O_{37}$
M_r	1845.82
Crystal description	Yellow prism
Crystal size /mm	0.30 × 0.21 × 0.12
Crystal system, space group	Triclinic, *P*-1
a /Å	11.5039(11)
b /Å	11.9145(10)
c /Å	14.6279(13)
α /°	74.687(4)
β /°	68.753(4)
γ /°	87.232(4)
Volume /Å^3	1799.8(3)
Z	1
$\rho_{calculated}$ /g cm^{-3}	1.703
$F(000)$	946
μ /mm^{-1}	0.678
θ range /°	3.78 to 28.28
Index ranges	$-15 \leq h \leq 13$ $-15 \leq k \leq 15$ $-19 \leq l \leq 19$
Reflections collected	60089
Independent reflections	8909 ($R_{int} = 0.0311$)
Final R indices [I>2σ(I)]	$R_1 = 0.0283$ $wR_2 = 0.0732$
Final R indices (all data)	$R_1 = 0.0326$ $wR_2 = 0.0755$
$\Delta\rho_{max}$ and $\Delta\rho_{min}$ /e.Å^{-3}	0.877 and −0.624

Table S2 Geometric information (distances in Å and angles in degrees) for the O–H$\cdots$A hydrogen bond interactions of the compound $2[MoO_2Cl_2(H_2O)_2]\cdot(C_{36}H_{36}N_{24}O_{12})\cdot17H_2O\cdot2HCl$ (**2**).[a]

C–H$\cdots$A	***d*(H$\cdots$A)**	***d*(O$\cdots$A)**	**∠(OHA)**
O1W–H1W$\cdots$O5^{ii}	1.966(11)	2.8088(18)	170(2)
O1W–H2W$\cdots$O3W	1.781(10)	2.624(2)	173(3)
O2W–H3W$\cdots$O4W^{ii}	2.017(16)	2.7898(19)	151(2)
O2W–H4W$\cdots$O4W	1.905(11)	2.743(2)	171(3)
O3W–H5W$\cdots$Cl3^{iii}	2.327(12)	3.1625(16)	166(3)
O3W–H6W$\cdots$O7W^{iv}	2.080(18)	2.857(2)	152(3)
O4W–H7W$\cdots$Cl3	2.244(10)	3.0815(14)	172(2)
O4W–H8W$\cdots$O4	1.995(12)	2.7990(18)	159(2)
O5W–H9W$\cdots$O7	1.800(11)	2.6316(19)	168(3)
O5W–H10W$\cdots$O6W	1.880(11)	2.716(2)	172(3)
O6W–H11W$\cdots$O6	1.879(14)	2.6972(19)	160(3)
O6W–H12W$\cdots$Cl3^{v}	2.290(10)	3.1349(16)	174(3)
O7W–H13W$\cdots$O4^{i}	2.42(2)	2.9891(19)	125(2)
O7W–H13W$\cdots$O5^{i}	2.251(19)	2.9034(18)	134(2)
O7W–H14W$\cdots$O6W	1.908(13)	2.730(2)	160(3)
O8W–H15W$\cdots$O3^{i}	2.007(18)	2.7019(19)	140(2)
O8W–H15W$\cdots$O4^{i}	2.54(2)	3.000(2)	115(2)
O8W–H16W$\cdots$O7W	1.838(10)	2.678(2)	175(3)
O9W–H17W$\cdots$O8	1.844(16)	2.6139(19)	155(3)
O9W–H18W$\cdots$O5W	1.654(11)	2.483(3)	175(3)

[a] Symmetry transformations used to generate equivalent atoms: (i) $-x+1, -y+1, z+1$; (ii) $-x+1, -y+2, -z$; (iii) $x-1, y, z$; (iv) $-x, -y+1, -z+1$; (v) $x-1, y-1, z+1$.

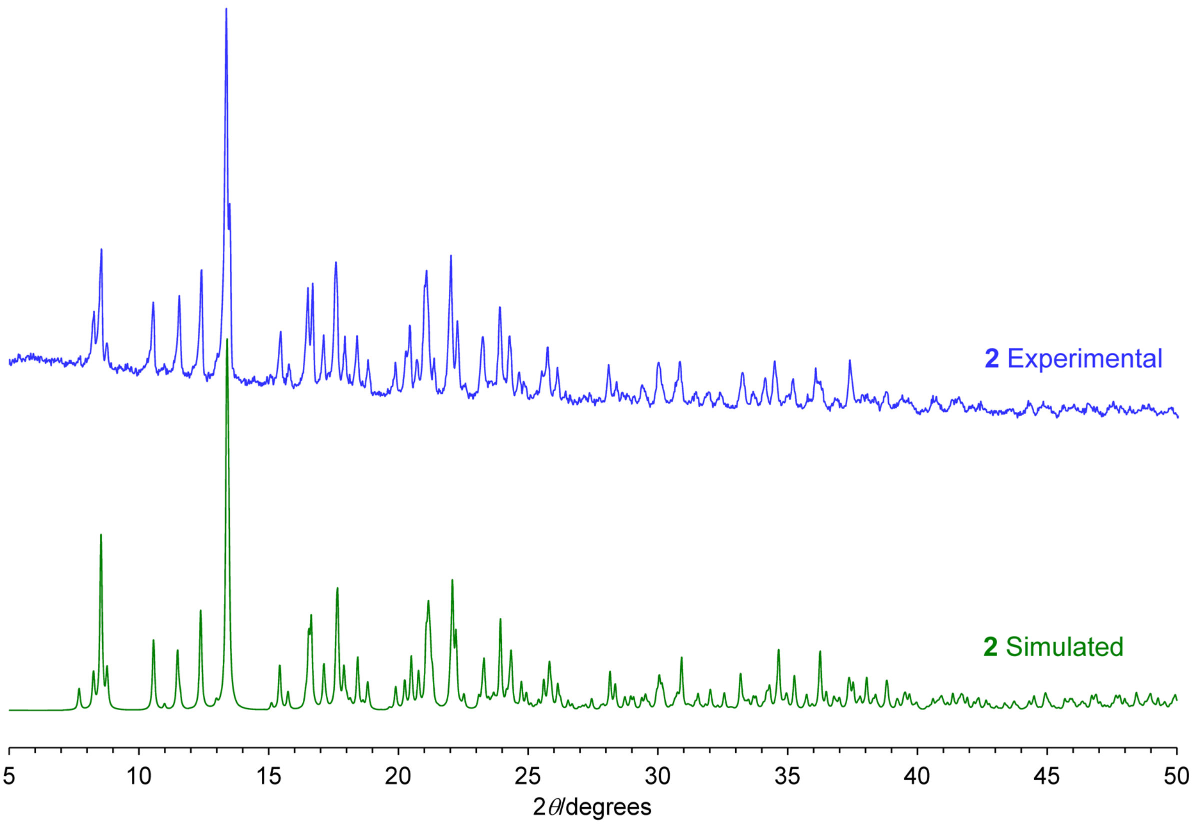

Fig. S1 Experimental powder X-ray diffraction pattern of **2** compared with the simulated pattern calculated from the crystal structure data reported in this paper for $2[MoO_2Cl_2(H_2O)_2]\cdot(C_{36}H_{36}N_{24}O_{12})\cdot17H_2O\cdot2HCl$.

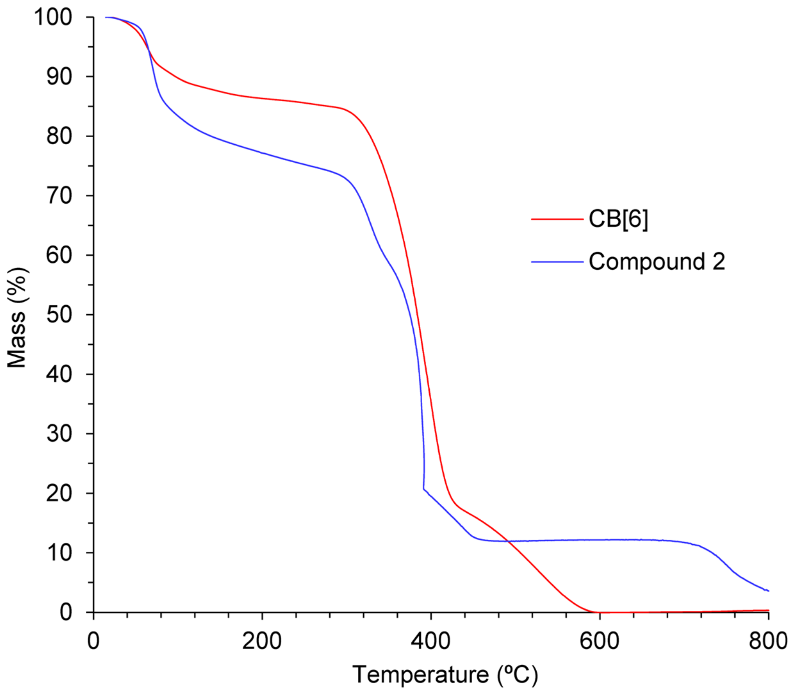

Fig. S2 TGA curves of the starting material CB[6] and the supramolecular adduct **2**.

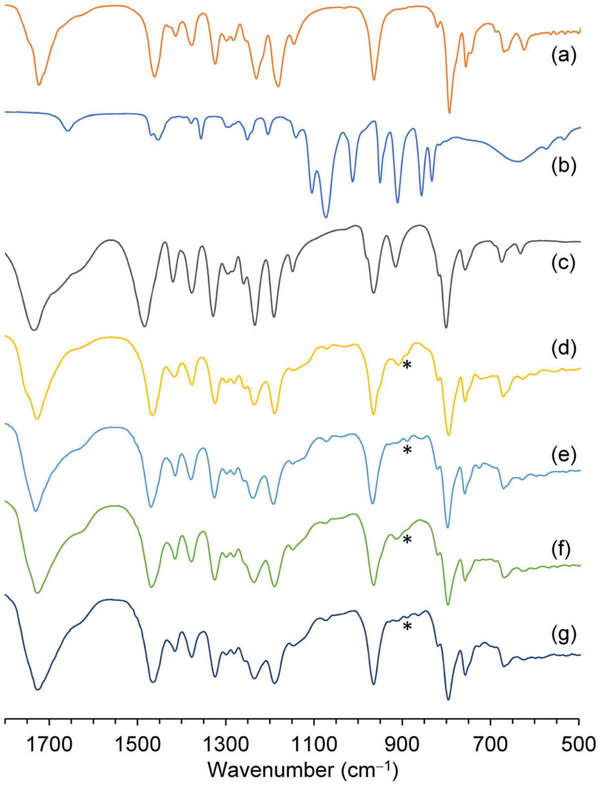

Fig. S3 ATR FT-IR spectra of (a) CB[6], (b) complex **1**, (c) compound **2**, and the solids recovered from the reactions (d) **2**/Cy$_8$/H_2O_2/MeCN/70 °C, (e) **2**/Sty/H_2O_2/MeCN/70 °C, (f) **2**/Cy$_8$/H_2O_2/EtOH/90 °C, and (g) **2**/Sty/H_2O_2/EtOH/70 °C. The asterisk denotes a new band not observed for **2**.

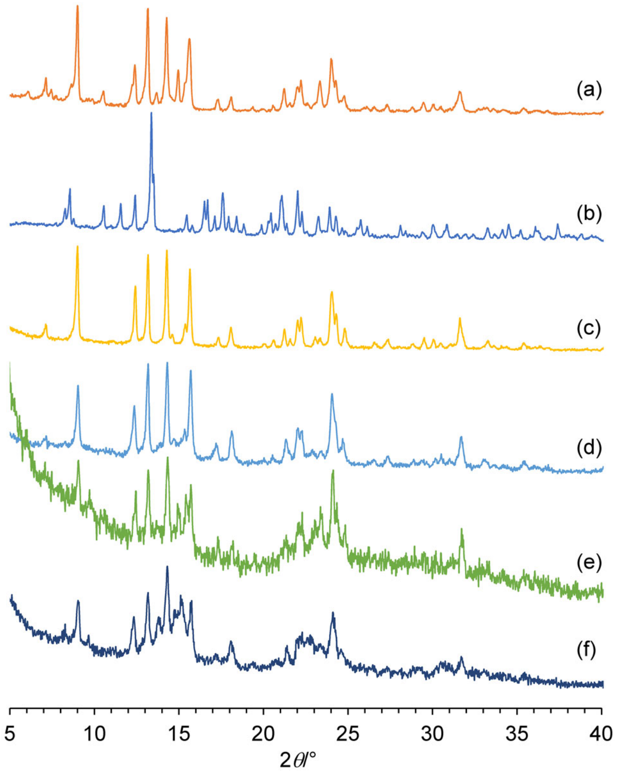

Fig. S4 PXRD patterns of (a) CB[6], (b) compound **2**, and the solids recovered from the reactions (c) **2**/Cy$_8$/H_2O_2/MeCN/70 °C, (d) **2**/Sty/H_2O_2/MeCN/70 °C, (e) **2**/Cy$_8$/H_2O_2/EtOH/90 °C, and (f) **2**/Sty/H_2O_2/EtOH/70 °C.

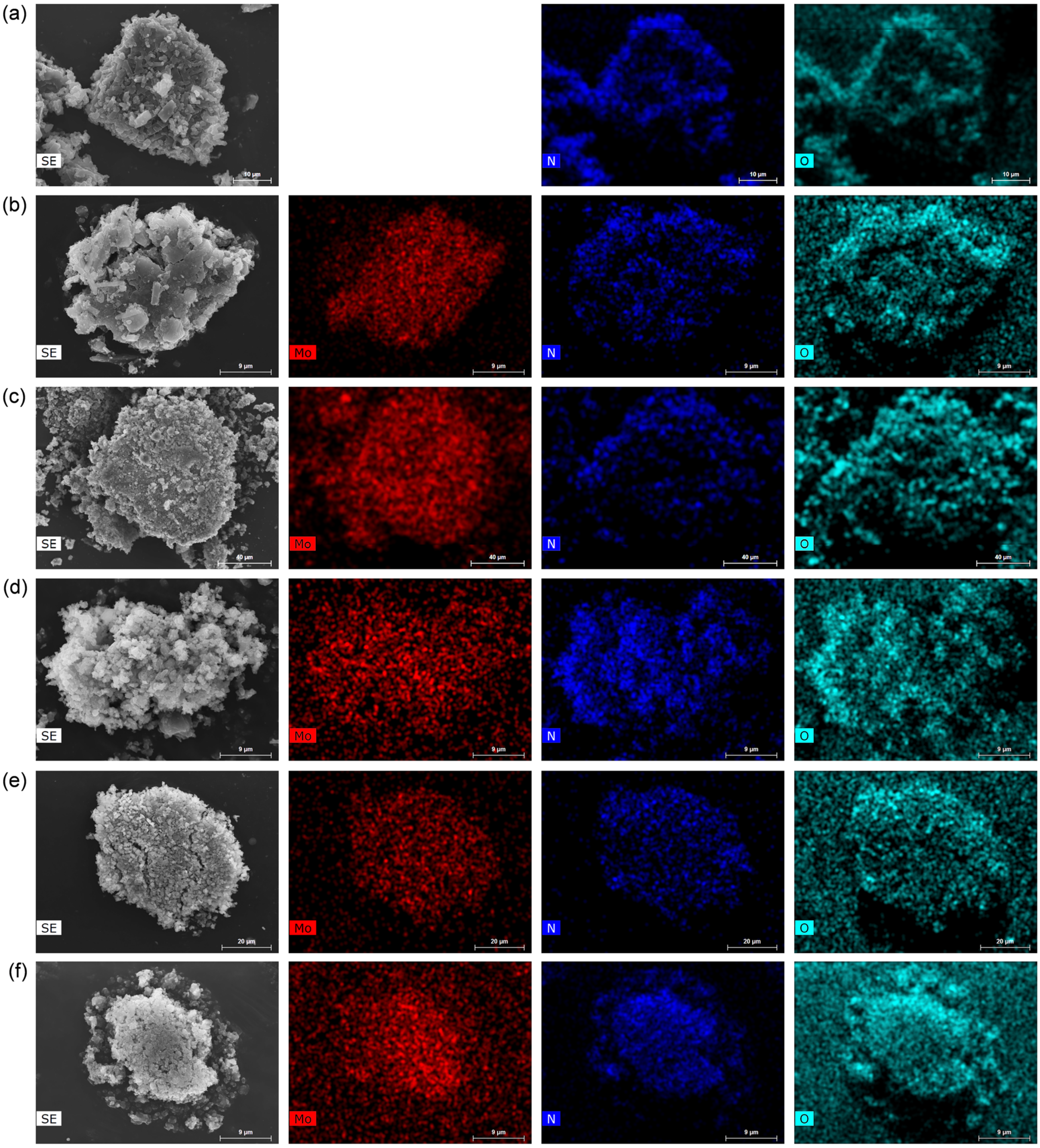

Fig. S5 SEM images and corresponding EDS Mo/N/O mapping images of (a) CB[6], (b) compound **2**, and the solids recovered from the reactions (c) **2**/Cy8/H_2O_2/MeCN/70 °C, (d) **2**/Sty/H_2O_2/MeCN/70 °C, (e) **2**/Cy8/H_2O_2/EtOH/90 °C, and (f) **2**/Sty/H_2O_2/EtOH/70 °C.

Mass spectral data for selected products

2-Ethoxycyclooctanone [(Cy$_8$(=O)(OEt)], m/z (relative intensity): 170 [M+] (2), 169 (8), 156 (9), 155 (79), 127 (9), 110 (10), 109 (100), 97 (8), 83 (16), 81 (17), 67 (60), 57 (12), 55 (24), 43 (18), 41 (14), 39 (7), 29 (9).

2-Butoxycyclooctanone [(Cy$_8$(=O)(OBu)], m/z (relative intensity): 198 [M+] (1), 197 (5), 156 (9), 155 (79), 127 (9), 110 (10), 109 (100), 97 (3), 83 (8), 81 (12), 67 (51), 57 (7), 55 (17), 43 (8), 41 (10), 39 (3), 29 (3).

2-Methoxycyclooctanol [Cy$_8$(OH)(OMe)], m/z (relative intensity): 158 [M+] (0.8), 144 (1), 143 (13), 128 (3), 127 (8), 126 (8), 125 (29), 112 (4), 109 (6), 108 (11), 99 (2), 98 (15), 97 (21), 93 (18), 87 (3), 85 (11), 83 (17), 82 (25), 79 (12), 76 (6), 72 (8), 71 (100), 70 (18), 69 (10), 67 (18), 66 (2), 61 (1), 59 (6), 58 (16), 57 (13), 55 (16), 54 (4), 51 (1), 45 (10), 43 (7), 41 (13), 39 (4).

2-Ethoxycyclooctanol [Cy$_8$(OH)(OEt)], m/z (relative intensity): 172 [M+] (1), 155 (0.3), 143 (22), 141 (16), 126 (8), 125 (46), 110 (10), 108 (11), 99 (15), 97 (15), 93 (15), 85 (100), 82 (32), 81 (27), 79 (26), 72 (12), 70 (16), 67 (22), 57 (61), 55 (30), 44 (16), 43 (22), 41 (29).

2-Butoxycyclooctanol [Cy$_8$(OH)(OBu)], m/z (relative intensity): 200 [M+] (1.6), 170 (4), 169 (18), 159 (7), 143 (30), 126 (15), 125 (74), 113 (38), 109 (26), 97 (34), 93 (26), 85 (20), 83 (44), 82 (56), 79 (40), 70 (36), 67 (42), 57 (100), 55 (56), 43 (22), 41 (52). 39 (10), 29 (12), 18 (14).

2-Dimethoxycyclooctane [Cy$_8$(OMe)$_2$], m/z (relative intensity): 172 [M+] (8), 171 (82), 143 (2), 142 (11), 140 (3), 139 (22), 137 (100), 130 (8), 129 (100), 128 (8), 127 (5), 125 (2), 121 (1), 115 (3), 114 (13), 111 (22), 110 (19), 109 (3), 102 (1), 101 (8), 100 (3), 99 (4), 98 (7), 97 (78), 96 (7), 95 (5), 94 (2), 93 (5), 92 (2), 91 (2), 88 (6), 87 (50), 86 (1), 85 (8), 84 (14), 83 (48), 82 (18), 81 (10), 79 (6), 75 (6), 74 (88), 73 (14), 71 (6), 70 (8), 69 (90), 68 (20), 67 (14), 59 (50), 57 (6), 56 (12), 55 (72), 54 (8), 53 (8), 45 (8), 43 (30), 42 (11), 41 (31), 39 (9), 29 (4), 28 (4), 27 (3), 18 (2), 15 (3).

2-Hydroxycyclooctanone [Cy$_8$(=O)OH], m/z (relative intensity): 142 [M+] (8), 125 (6), 124 (54), 109 (6), 99 (6), 98 (42), 97 (12), 96 (28), 95 (38), 82 (18), 81 (60), 80 (40), 71 (16), 70 (16), 68 (38), 67 (30), 58 (8), 57 (100), 55 (28), 54 (11), 53 (7), 45 (3), 44 (14), 43 (13), 42 (12), 41 (20), 39 (10), 31 (2), 29 (4), 27 (3).

1,2-Cyclooctanedione [Cy$_8$(=O)$_2$], m/z (relative intensity): 141 [M+1]+ (6), 140 (66), 112 (16), 98 (22), 97 (18), 84 (54), 83 (28), 70 (12), 69 (44), 68 (100), 67 (12), 56 (36), 55 (86), 43 (8), 42 (20), 41 (30), 39 (13), 28 (4).

1,2-Cyclohexanediol [Cy$_6$(OH)$_2$], m/z (relative intensity): 116 [M+] (10), 99 (4), 98 (43), 97 (17), 83 (44), 80 (10), 70 (100), 69 (26), 67 (8), 57 (38), 55 (13), 44 (12), 41 (12), 39 (6), 29 (2).

Ethoxycyclohexanol [Cy$_6$(OH)(OEt)], m/z (relative intensity): 144 [M+] (18); 127 (1.2), 126 (2.2), 115 (6), 111 (1.6), 98 (39), 97 (26), 85 (100), 82 (68), 81 (20), 70 (68), 69 (22), 57 (44). 55 (10), 43 (10), 41 (17), 39 (5), 29 (4).

1-Phenyl-1,2-ethanediol (styrene glycol) [Sty(OH)$_2$], m/z (relative intensity): 138 [M+] (6), 120 (0.6), 108 (9), 107 (100), 91 (8), 79 (61), 77 (48), 65 (3), 51 (6).

References

1 F. J. Arnaiz, R. Aguado, J. Sanz-Aparicio and M. Martinez-Ripoll, *Polyhedron*, 1994, **13**, 2745-2749.

2 J. Kim, I.-S. Jung, S.-Y- Kim, E. Lee, J.-K. Kang, S. Sakamoto, K. Yamaguchi and K. Kim, *J. Am. Chem. Soc.*, 2000, **122**, 540-541.

3 A. Day, A. P. Arnold, R. J. Blanch and B. Snushall, *J. Org. Chem.*, 2001, **66**, 8094-8100.

4 T. Kottke and D. Stalke, *J. Appl. Crystallogr.*, 1993, **26**, 615-619.

5 APEX2, *Data Collection Software*, version 2012.4, Bruker AXS, Delft, The Netherlands, 2012.

6 Cryopad, *Remote monitoring and control*, version 1.451, Oxford Cryosystems, Oxford, United Kingdom, 2006.

7 SAINT+, *Data Integration Engine*, version 8.27b©, Bruker AXS, Madison, Wisconsin, USA, 1997-2012.

8 G. M. Sheldrick, SADABS 2012/1, *Bruker AXS Area Detector Scaling and Absorption Correction Program*, Bruker AXS, Madison, Wisconsin, USA, 2012.

9 G.M. Sheldrick, *Acta Crystallogr. Sect. A: Found. Adv.*, 2008, **64**, 112-122.

10 G.M. Sheldrick, SHELXT-2014, *Program for Crystal Structure Solution*, University of Göttingen, 2014.

11 G.M. Sheldrick, SHELXL v. 2014/3, *Program for Crystal Structure Refinement*, University of Göttingen, 2014.